

Supporting Information for ”A data-driven approach to physics-based risk models for deep-seated landslides”

Rachael Lau¹, Manolis Veveakis¹

¹Duke University, Durham, NC 27708

Contents of this file

1. Sentinel-1 InSAR Interferogram Files for Time Series Inversion
2. Field-model Temperature Comparison Plots
3. Sample InSAR - Model Displacement Comparison Plots for Samples 1-5

Introduction This document serves as the supporting information for our study, providing detailed supplementary datasets and visualizations crucial for a comprehensive understanding of our methodologies and findings. The contents within aim to enhance the transparency and accessibility of our research, ensuring that fellow researchers can validate and build upon our work effectively. Included are the Sentinel-1 InSAR interferogram files that form the backbone of our time series inversion analysis and were downloaded from the Alaska Satellite Facility Vertex Platform. We also provide a series of comparison plots that juxtapose field measured temperatures with those predicted by our models. Lastly, for a more targeted analysis, we include InSAR model displacement comparison plots for five specific samples on the scarp. These plots compare the displacement data

derived from InSAR observations with those predicted by our models, providing a sample by sample breakdown of model performance.

Sentinel-1 InSAR Interferogram Files for Time Series Inversion

S1BB_20190503T174622_20190515T174622_VVP012_INT40_G_weF_4453
S1BB_20190503T174622_20190515T174622_VVP012_INT40_G_weF_D7F2
S1BB_20190503T174622_20190608T174624_VVP036_INT40_G_weF_4B41
S1BB_20190503T174622_20190620T174624_VVP048_INT40_G_weF_321D
S1BB_20190503T174622_20190702T174625_VVP060_INT40_G_weF_5E47
S1BB_20190515T174622_20190608T174624_VVP024_INT40_G_weF_9700
S1BB_20190515T174622_20190608T174624_VVP024_INT40_G_weF_E4F4
S1BB_20190515T174622_20190620T174624_VVP036_INT40_G_weF_0296
S1BB_20190515T174622_20190620T174624_VVP036_INT40_G_weF_39E4
S1BB_20190515T174622_20190702T174625_VVP048_INT40_G_weF_DE31
S1BB_20190515T174622_20190714T174626_VVP060_INT40_G_weF_EC4E
S1BB_20190608T174624_20190620T174624_VVP012_INT40_G_weF_55D5
S1BB_20190608T174624_20190620T174624_VVP012_INT40_G_weF_AD9C
S1BB_20190608T174624_20190702T174625_VVP024_INT40_G_weF_20EA
S1BB_20190608T174624_20190702T174625_VVP024_INT40_G_weF_A335
S1BB_20190608T174624_20190714T174626_VVP036_INT40_G_weF_3B0F
S1BB_20190608T174624_20190807T174627_VVP060_INT40_G_weF_5236
S1BB_20190620T174624_20190702T174625_VVP012_INT40_G_weF_9078
S1BB_20190620T174624_20190702T174625_VVP012_INT40_G_weF_D547
S1BB_20190620T174624_20190714T174626_VVP024_INT40_G_weF_5E5A

S1BB_20190620T174624_20190714T174626_VVP024.INT40.G_weF_B7AD
S1BB_20190620T174624_20190807T174627_VVP048.INT40.G_weF_7E4F
S1BB_20190620T174624_20190819T174628_VVP060.INT40.G_weF_366E
S1BB_20190702T174625_20190714T174626_VVP012.INT40.G_weF_3534
S1BB_20190702T174625_20190714T174626_VVP012.INT40.G_weF_A87D
S1BB_20190702T174625_20190807T174627_VVP036.INT40.G_weF_1E82
S1BB_20190702T174625_20190819T174628_VVP048.INT40.G_weF_995D
S1BB_20190702T174625_20190831T174629_VVP060.INT40.G_weF_F527
S1BB_20190714T174626_20190807T174627_VVP024.INT40.G_weF_0CB4
S1BB_20190714T174626_20190807T174627_VVP024.INT40.G_weF_29B7
S1BB_20190714T174626_20190819T174628_VVP036.INT40.G_weF_06D2
S1BB_20190714T174626_20190819T174628_VVP036.INT40.G_weF_4D92
S1BB_20190714T174626_20190831T174629_VVP048.INT40.G_weF_18F3
S1BB_20190714T174626_20190912T174629_VVP060.INT40.G_weF_BF35
S1BB_20190807T174627_20190819T174628_VVP012.INT40.G_weF_A178
S1BB_20190807T174627_20190819T174628_VVP012.INT40.G_weF_ACF3
S1BB_20190807T174627_20190831T174629_VVP024.INT40.G_weF_1E24
S1BB_20190807T174627_20190831T174629_VVP024.INT40.G_weF_C9AB
S1BB_20190807T174627_20190912T174629_VVP036.INT40.G_weF_3261
S1BB_20190807T174627_20191006T174630_VVP060.INT40.G_weF_6A58
S1BB_20190819T174628_20190831T174629_VVP012.INT40.G_weF_7E6B
S1BB_20190819T174628_20190831T174629_VVP012.INT40.G_weF_ECA4
S1BB_20190819T174628_20190912T174629_VVP024.INT40.G_weF_144C

S1BB_20190819T174628_20190912T174629_VVP024_INT40_G_weF_5A4C
S1BB_20190819T174628_20191006T174630_VVP048_INT40_G_weF_AB74
S1BB_20190819T174628_20191018T174630_VVP060_INT40_G_weF_918C
S1BB_20190831T174629_20190912T174629_VVP012_INT40_G_weF_4E75
S1BB_20190831T174629_20190912T174629_VVP012_INT40_G_weF_9E4A
S1BB_20190831T174629_20191006T174630_VVP036_INT40_G_weF_5A67
S1BB_20190831T174629_20191006T174630_VVP036_INT40_G_weF_C545
S1BB_20190831T174629_20191018T174630_VVP048_INT40_G_weF_42A8
S1BB_20190831T174629_20191030T174630_VVP060_INT40_G_weF_59E0
S1BB_20190912T174629_20191006T174630_VVP024_INT40_G_weF_44ED
S1BB_20190912T174629_20191006T174630_VVP024_INT40_G_weF_778F
S1BB_20190912T174629_20191018T174630_VVP036_INT40_G_weF_DA12
S1BB_20190912T174629_20191030T174630_VVP048_INT40_G_weF_188A
S1BB_20190912T174629_20191111T174630_VVP060_INT40_G_weF_9EF5
S1BB_20191006T174630_20191018T174630_VVP012_INT40_G_weF_7B0F
S1BB_20191006T174630_20191018T174630_VVP012_INT40_G_weF_A106

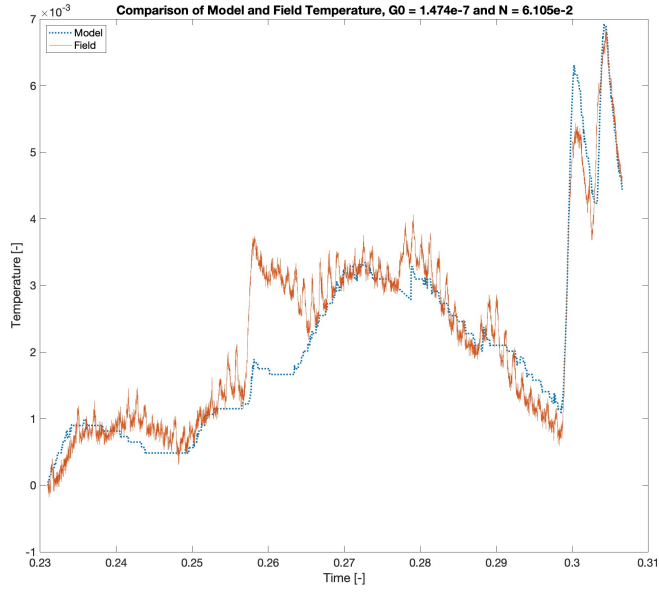


Figure S1. Comparison of model-output temperature with in situ temperature for Option C1.

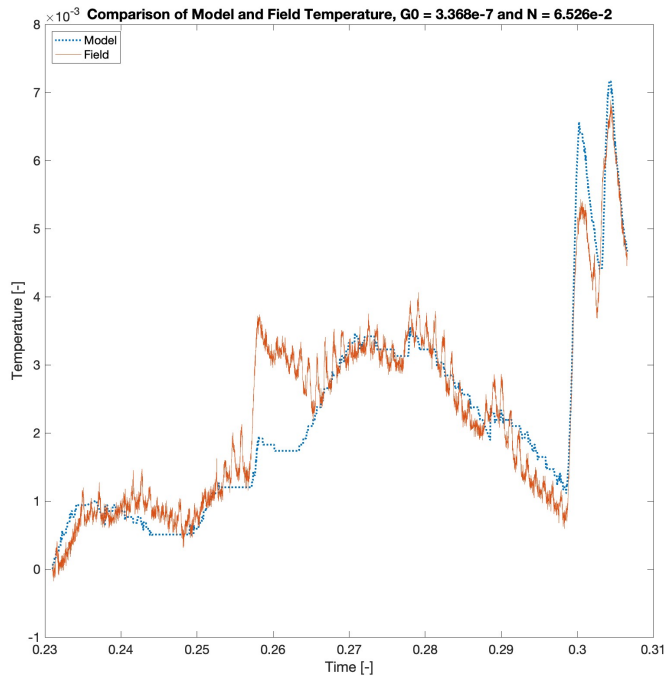


Figure S2. Comparison of model-output temperature with in situ temperature for Option C2.

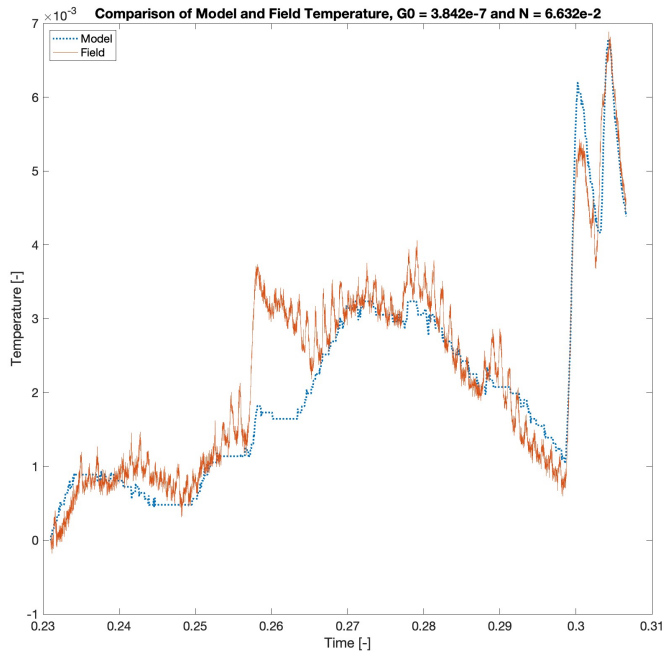


Figure S3. Comparison of model-output temperature with in situ temperature for Option C3.

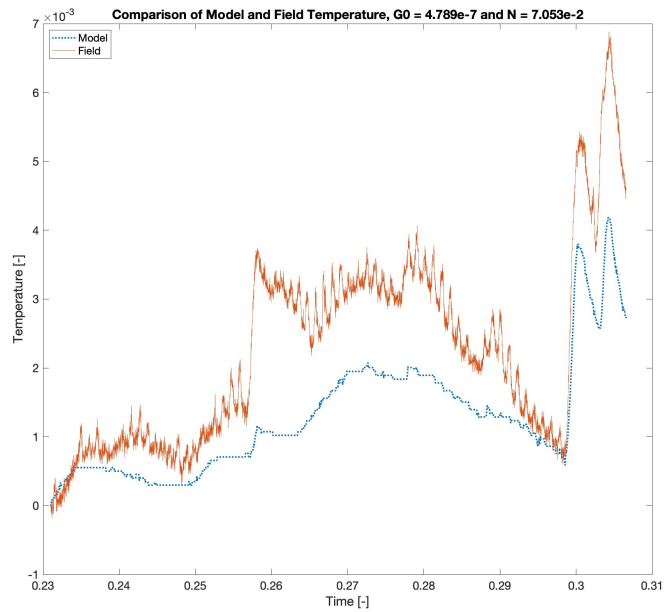


Figure S4. Comparison of model-output temperature with in situ temperature for Option C5.

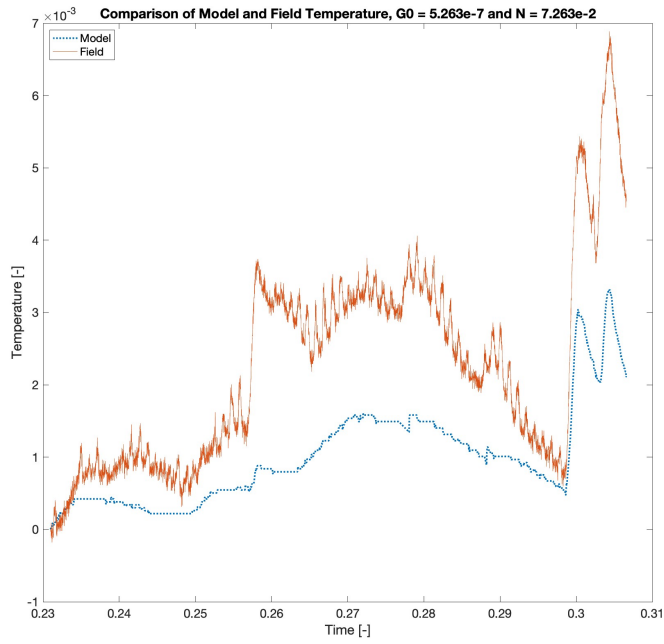


Figure S5. Comparison of model-output temperature with in situ temperature for Option C6.

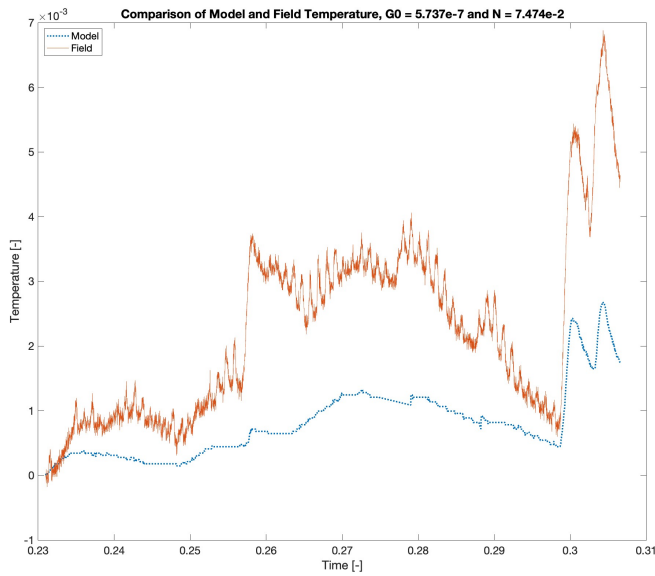


Figure S6. Comparison of model-output temperature with in situ temperature for Option C7.

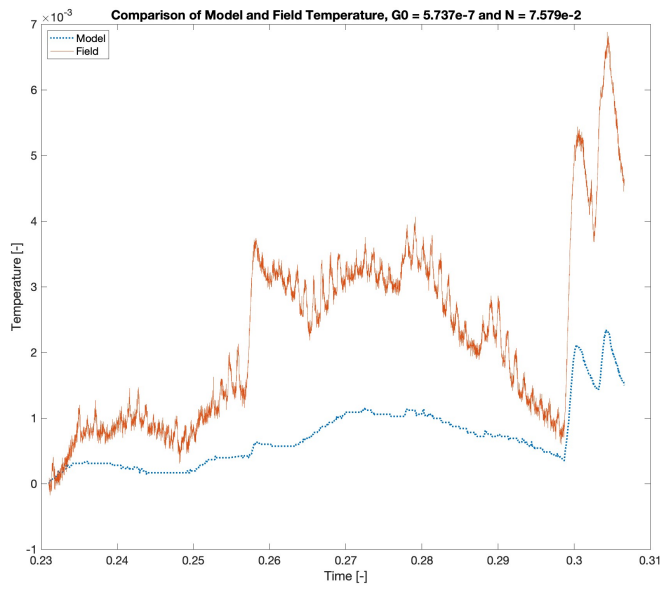


Figure S7. Comparison of model-output temperature with in situ temperature for Option C8.

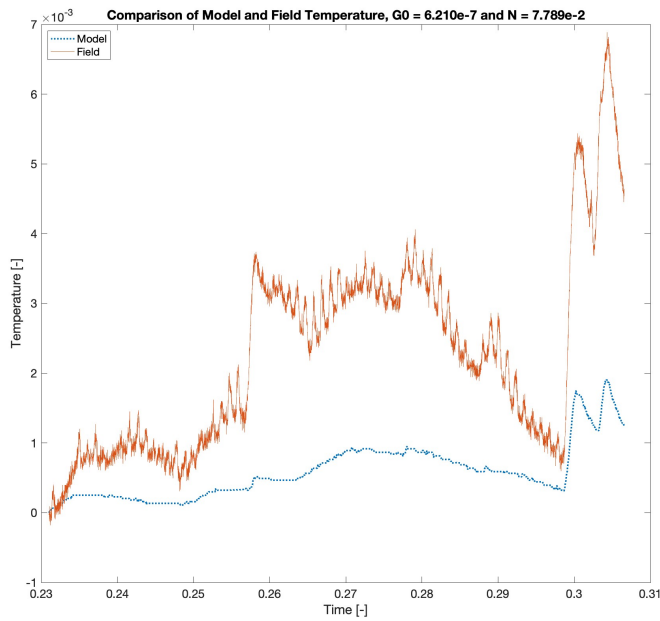


Figure S8. Comparison of model-output temperature with in situ temperature for Option C9.

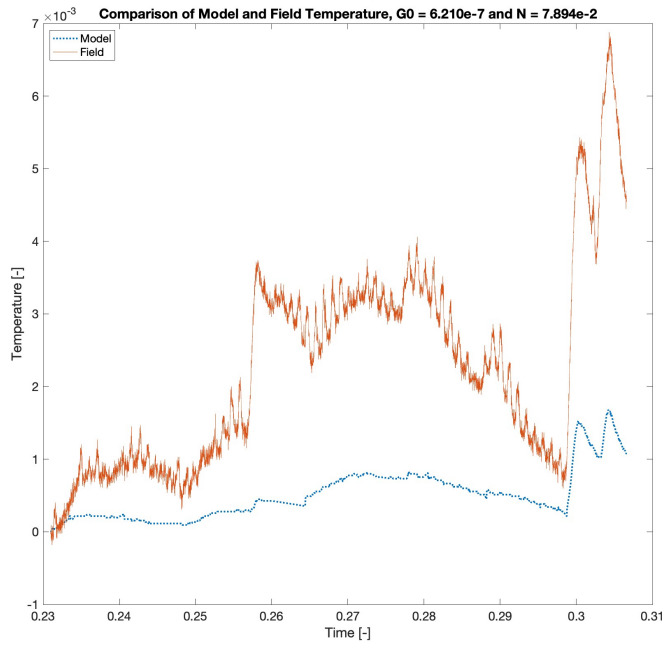


Figure S9. Comparison of model-output temperature with in situ temperature for Option C10.

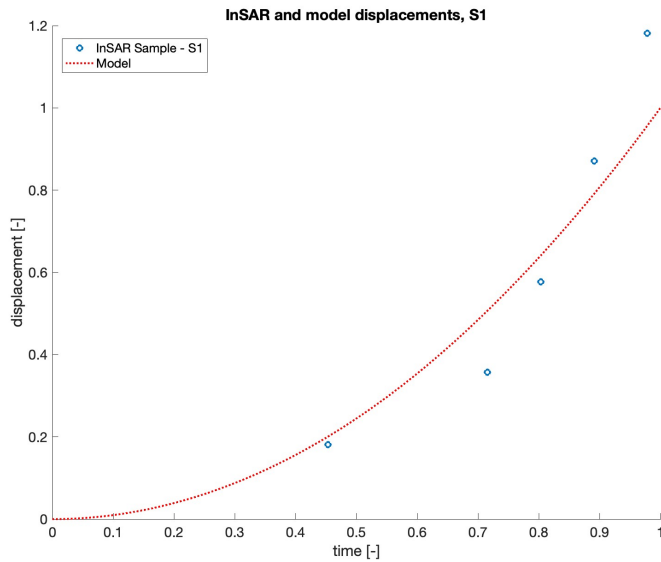


Figure S10. Comparison of model-output displacement for optimized S10 readings and correlated InSAR time series output for S1 sample pixel.

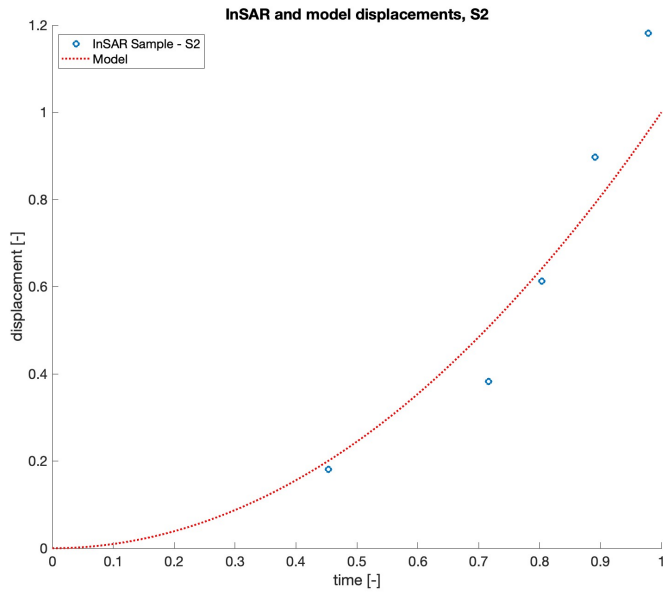


Figure S11. Comparison of model-output displacement for optimized S10 readings and correlated InSAR time series output for S2 sample pixel.

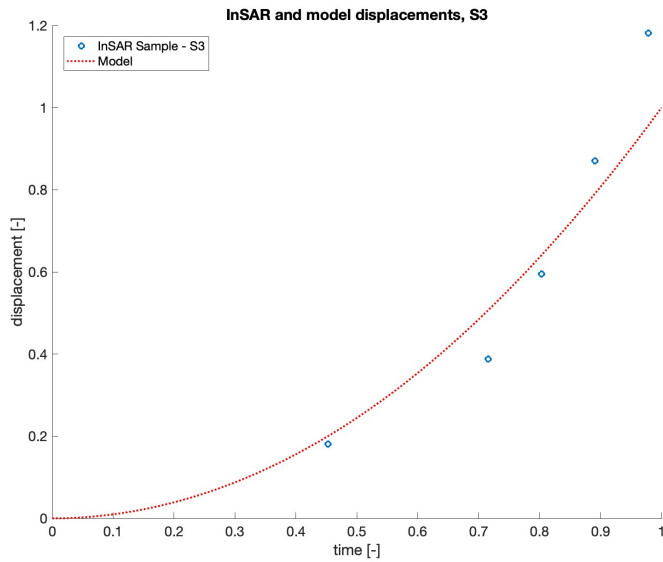


Figure S12. Comparison of model-output displacement for optimized S10 readings and correlated InSAR time series output for S3 sample pixel.

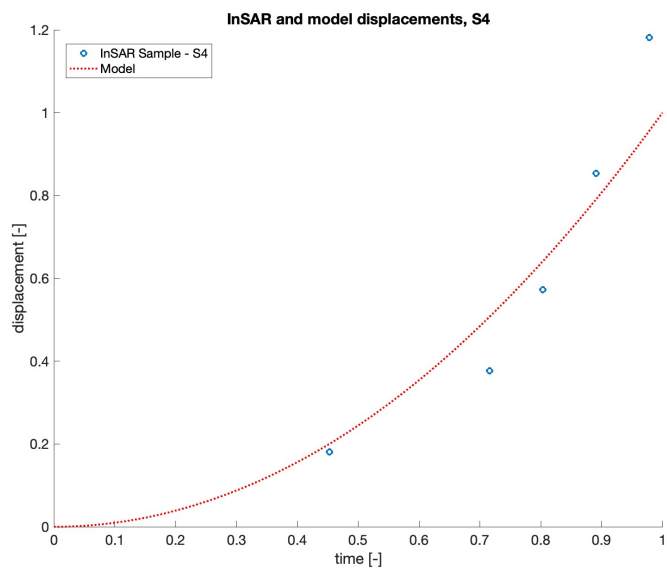


Figure S13. Comparison of model-output displacement for optimized S10 readings and correlated InSAR time series output for S4 sample pixel.

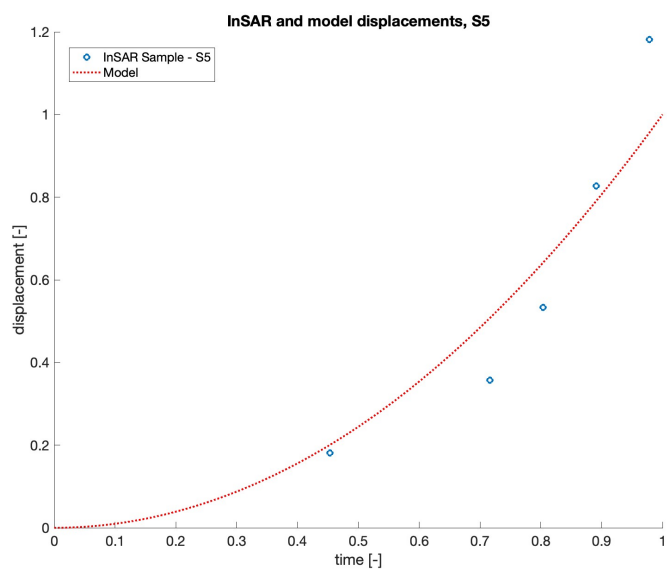


Figure S14. Comparison of model-output displacement for optimized S10 readings and correlated InSAR time series output for S5 sample pixel.